Borneo Journal of Pharmacy
Vol 9 Issue 1 March 2026
Pages 60 – 70

https://journal.umpr.ac.id/index.php/bjop/article/view/9356
DOI: https://doi.org/10.33084/bjop.v9i1.9356
e-ISSN: 2621-4814

Research Article

Synthesis of 4-Hydroxycinnamic Acid from Malonic Acid and 4-Hydroxybenzaldehyde as Starting Materials with the Variation of the Reflux Time

Iin Narwanti *

Fahmi Humaidi Abdillah

Department of Pharmacy, Universitas Ahmad Dahlan, Yogyakarta, Special Region of Yogyakarta, Indonesia

*email: iin.narwanti@pharm.uad.ac.id; phone: +6274563515

Keywords:
4-hydroxycinnamic acid
Condensation
Knoevenagel-Doebner
Reflux time variation

Abstract

Cinnamic acid derivatives, naturally occurring compounds found in plants and also synthetically produced, exhibit diverse biological activities, including antioxidant, antiplasmodial, tyrosinase-inhibitory, antibacterial, anti-inflammatory, antitumor, and anticancer properties, with 4-hydroxycinnamic acid representing a particularly valuable derivative for pharmaceutical development. However, the successful synthesis of these compounds requires careful optimization of reaction conditions, particularly the reflux time, which must balance complete reactant conversion against product degradation that may occur with excessive heating to achieve maximum yield and purity. This study aimed to optimize the reaction yield in the synthesis of 4-hydroxycinnamic acid by varying the reflux time. 4-Hydroxycinnamic acid was synthesized via a reaction between malonic acid and 4-hydroxybenzaldehyde using pyridine-piperidine as a catalyst. The reflux time was varied at 3, 5, and 7 hours. The mixture was refluxed at 70–80°C with constant stirring at 900 rpm. After the reaction, the crude product was recrystallized and dried, and the yield was calculated. TLC was employed to compare the product's R_f value with that of the starting material using various eluents. Furthermore, the synthesized product was characterized by Fourier-Transform Infrared and Nuclear Magnetic Resonance spectroscopy to elucidate its structure. The results revealed that the average yields at reflux times of 3, 5, and 7 hours were 58.6, 66.78, and 63.87%, respectively, with the optimal yield achieved at 5 hours. Physicochemical and spectral data confirmed that the obtained product was 4-hydroxycinnamic acid. Purity analysis showed that the synthesized compound had a purity level of 95%.

Received: February 9th, 2025
1st Revised: October 28th, 2025
Accepted: December 11th, 2025
Published: March 30th, 2026

INTRODUCTION

Cinnamic acid and its structural derivatives constitute a vital class of phenylacrylic acid organic compounds that occur naturally and are distributed abundantly throughout the plant kingdom[1]. Characterized by an α,β-unsaturated carboxylic acid core framework, cinnamic acid serves as a fundamental biosynthetic precursor for flavonoids, coumarins, and an array of other downstream biologically active macromolecules. Owing to their versatile structural architecture and remarkable pharmacological profiles, cinnamoyl-bearing compounds are widely recognized as privileged scaffolds in medicinal chemistry, sparking intense research interest into their therapeutic potential. Beyond their extensive biomedical applications, these molecules are commercially indispensable across the cosmetic sector[2], the food and nutraceutical industries[3], and

How to cite: Narwanti I, Abdillah FH. Synthesis of 4-Hydroxycinnamic Acid from Malonic Acid and 4-Hydroxybenzaldehyde as Starting Materials with the Variation of the Reflux Time. Borneo J Pharm. 2026;9(1):60-70. doi:10.33084/bjop.v9i1.9356

fragrance or perfume manufacturing[4] due to their diverse biological properties, which include documented antioxidant[5,6], antiplasmodial[7], tyrosinase-inhibiting[8], antibacterial[9], anti-inflammatory[1,10], antitumor[11,12], and anticancer[13] activities.

To meet industrial and research needs, various classical synthetic methodologies have been established for preparing cinnamic acid and its analogs, most notably the Perkin reaction[14], the Claisen-Schmidt condensation[15], the Knoevenagel condensation[16,17], and specialized enzymatic pathways[18]. The traditional Perkin reaction, for instance, drives the condensation of an aromatic aldehyde and an acid anhydride using an alkali salt catalyst[19]; however, this pathway often requires harsh reaction conditions and sustained high temperatures, which can trigger unwanted side reactions or decompose sensitive reactants. Alternatively, the Claisen-Schmidt condensation involves the reaction of aldehydes with acetates followed by alkaline hydrolysis to yield the desired cinnamic esters. While Hatsuda *et al*.[15] successfully optimized an (*E*)-cinnamic acid derivative protocol via a sodium metal-mediated Claisen-Schmidt condensation using a methanol-toluene solvent system, multi-step ester hydrolyses remain vulnerable to competitive pathways, such as the Cannizzaro side reaction, which can compromise overall product purity. Conversely, the Knoevenagel condensation is often preferred in modern laboratories because it operates under significantly milder conditions and provides superior product yields. Other strategies, such as the protocol developed by Chiriac and colleagues employing a 4-dimethylaminopyridine (DMAP)-pyridine base and boron tribromide (BBr_3) chemical agent, successfully generate cinnamic acid analogs in moderate yields; nonetheless, this methodology is constrained by high temperature requirements and prolonged reaction durations spanning 8 to 12 hours[20].

While these established frameworks offer diverse synthetic entry points, meticulous optimization of reaction conditions remains paramount to maximize overall synthesis efficiency and economic viability. Achieving a successful synthesis requires balancing the conversion rate of the starting materials against the thermal degradation of the product, a dynamic heavily governed by the precise regulation of the reflux duration. Consequently, the design of highly efficient, environmentally benign, and cost-effective synthetic pathways for functionalized cinnamoyl architectures remains a driving focus in organic synthesis. To address these parameters, the present study aims to synthesize 4-hydroxycinnamic acid by systematically investigating the effects of reaction time. Our approach focuses on identifying the optimal reflux duration to achieve maximum product yield under moderate, energy-efficient operating conditions. Furthermore, particular emphasis is placed on advancing greener synthetic methodologies by minimizing the consumption of hazardous organic solvents, directly aligning the workflow with sustainable chemistry practices. The structural identity of the synthesized 4-hydroxycinnamic acid was comprehensively validated by thin-layer chromatography (TLC), Fourier-transform infrared spectroscopy (FTIR), and nuclear magnetic resonance (NMR) spectroscopy, and its final purity profile was rigorously evaluated by High-Performance Liquid Chromatography (HPLC).

MATERIALS AND METHODS

Materials

The chemical reagents utilized in this study were of analytical grade and procured from standard commercial sources without further purification. The inventory comprised malonic acid, 4-hydroxybenzaldehyde, pyridine, piperidine, chloroform, n-hexane, glacial acetic acid, concentrated hydrochloric acid (HCl), ethanol, ethyl acetate, acetone, petroleum ether, dimethyl sulfoxide (DMSO), and distilled water. Experimental reaction monitoring and initial purity evaluations were conducted using TLC. The melting point profile of the isolated synthesis product was determined using an SMP3 melting point apparatus. Functional group characterization was performed via FTIR spectroscopy. Structural elucidation was achieved using NMR spectroscopy, including proton (^{1}H-NMR) and carbon (^{13}C-NMR) configurations, recorded on an Agilent DD2 spectrometer operating at 300 MHz and 500 MHz, respectively. For the NMR data, chemical shifts (δ) are reported in ppm relative to the residual solvent signals, while coupling constants (J values) are expressed in Hertz (Hz). The final product purity and specific retention times were evaluated using an Agilent 1260 Infinity II HPLC system (Agilent Technologies, Germany) equipped with a Dikma Diamonsil C-18 stationary phase column (5 µm, 150 x 4.6 mm). The chromatographic separation was carried out with an injection volume of 20 µL, a constant mobile-phase flow rate of 0.5 mL/minute, and an eluent system consisting of acetonitrile and water containing 10 mM ammonium chloride and 1.0% formic acid. All analytical samples evaluated by HPLC were prepared in DMSO as the dissolution medium.

Methods

Condensation and reflux optimization sequence

The synthesis of 4-hydroxycinnamic acid was initiated by introducing 520.3 mg (5.0 mmol) of malonic acid into a round-bottom flask, followed immediately by the addition of 2.0 mL of pyridine as the initial reaction solvent. This primary mixture was heated gently and continuously with agitation until the solid malonic acid was completely dissolved in the solvent. Subsequently, 305 mg (2.5 mmol) of 4-hydroxybenzaldehyde and 1 mL of piperidine were introduced to the solution to serve as the catalyst mixture. The combined reaction matrix was then brought to a stable, continuous reflux maintained at an operational temperature range of 70-80°C. To systematically evaluate the direct effect of reaction duration on total product conversion efficiency, the reflux processing time was varied at fixed experimental intervals of 3, 5, and 7 hours.

Precipitation and isolation protocol

Upon the completion of each respective heating period, the reaction flask was removed from the heat source and allowed to cool naturally to room temperature. The cooled mixture was then neutralized via the systematic, dropwise addition of 25.0 mL of 2.0 M HCl, which altered the solution properties and initiated the formation of a distinct, dense white precipitate. To optimize crystal growth dynamics and maximize the total recovery of the solid product, the round-bottom flask housing the suspension was transferred to an ice bath for localized thermal stabilization. The resulting crude solid was collected by vacuum filtration using a Büchner funnel, washed thoroughly with 50 mL of chilled water to remove residual salts, then washed a second time with 20 mL of petroleum ether to strip away organic impurities, and dried under vacuum to isolate the desired 4-hydroxycinnamic acid product.

Data analysis

Following the final drying stage, the total mass of the isolated crystalline solid was recorded on an analytical balance to determine the dry mass value required to calculate the final percentage yield of the synthesis. The obtained 4-hydroxycinnamic acid was then subjected to multi-instrumental data tracking to establish its chemical profile and verify final purity levels. Structural confirmation data were acquired by evaluating specific retention times on an Agilent 1260 Infinity II HPLC system, while functional group profiles were mapped by analyzing FTIR spectra. Final molecular confirmation was achieved by analyzing δ and J values from ^{1}H-NMR and ^{13}C-NMR spectra, which were evaluated alongside mobile-phase verification metrics and TLC migration maps to confirm overall product homogeneity.

RESULTS AND DISCUSSION

Piperidine serves as an effective organic base catalyst in the Knoevenagel-Doebner reaction, driving the strategic transformation of diverse aromatic aldehydes. A defining structural modification characterizing the Knoevenagel-Doebner pathway relative to the standard Knoevenagel condensation involves substituting diethyl malonate with an organic diacid framework[21]. Although classic historical designs by Doebner evaluated a broad range of aliphatic diacids, malonic acid remains the most widely deployed diacid component within contemporary synthetic schemes[22]. Mechanistically, the reaction initiates via a piperidine-facilitated chain elongation step, which is followed by a pyridine-mediated decarboxylation sequence that strips carboxyl functions from the intermediate diacid. The principal objective of this study was to optimize the reflux duration governing the condensation of 4-hydroxybenzaldehyde with malonic acid, as illustrated in **Figure 1**. Within this chemical environment, pyridine served as both a solvent matrix and a weak base, and the conversion was accelerated by using a small catalytic amount of piperidine.

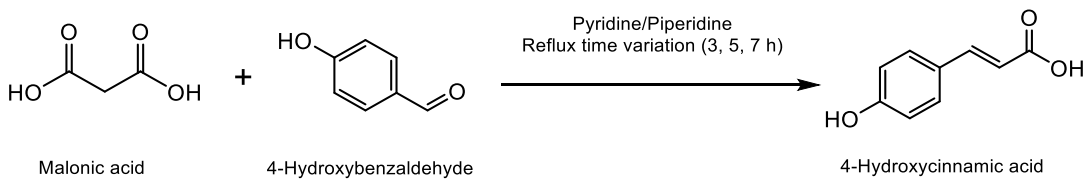

Figure 1. Synthesis of 4-hydroxycinnamic acid from malonic acid and 4-hydroxybenzaldehyde using pyridine-piperidine catalyst under varying reflux times.

The condensation reaction linking 4-hydroxybenzaldehyde and malonic acid successfully produced 4-hydroxycinnamic acid. The corresponding mass yields of the isolated 4-hydroxycinnamic acid compiled across the varied reflux intervals (3, 5, and 7 hours) are presented in **Table I**. The calculated percentage yields across the 3-, 5-, and 7-hour intervals were 58.6% ± 2.89, 66.78% ± 3.52, and 63.87% ± 1.29, respectively. These quantitative trends demonstrate that maintaining the reaction matrix under reflux for 5 hours establishes the optimal kinetic ceiling necessary to achieve the maximum yield of the target molecule. In comparison, a previously reported alternative synthesis of 4-hydroxycinnamic acid using a standalone diethylamine catalyst exhibited poor catalytic efficacy, yielding yields below 10%[23]. Similarly, separate historical methods utilizing microwave-assisted Knoevenagel-Doebner protocols with piperidine in dimethylformamide (DMF) at 90°C achieved moderate-to-good yields of phenolic acids within a compressed 30-minute reaction window[24]. In the present study, the binary pyridine-piperidine catalytic system, under standard 5-hour thermal reflux, successfully generated 4-hydroxycinnamic acid with an isolation yield exceeding 65%.

Table I. Isolated 4-hydroxycinnamic acid with various reflux times (3, 5, and 7 hours).

Group	Replication	Isolated product	Average Yield (%)
I	1	136.7	58.6±2.89
	2	155.1	
	3	163.4	
II	1	177.1	66.78±3.52
	2	189.3	
	3	145.3	
III	1	154.3	63.87±1.29
	2	121.6	
	3	197.0	

As collated in **Table II** and visualized in TLC migration maps in **Figure 2**, the observed retention factors (R_f) fluctuated in accordance with individual molecular polarities and the specific mobile phase compositions used. Adjustments in eluent polarity, along with competitive affinities between the mobile phase and the silica gel stationary phase, directly govern total compound migration. For instance, the R_f indicators tracking the starting precursors and the resulting 4-hydroxycinnamic acid decreased markedly when developed inside a lower-polarity eluent system consisting of *n*-hexane and ethyl acetate (2:1). Conversely, compound migration accelerated, yielding higher R_f outputs, when the structural polarity of the mobile phase was enhanced by introducing a multi-component system of chloroform, acetone, and acetic acid (10:5:0.5).

Table II. R_f values of malonic acid, 4-hydroxybenzaldehyde, and 4-hydroxycinnamic acid when developing with different eluents.

Compounds	R_f values		
	Eluent I	Eluent II	Eluent III
Malonic acid	0.025	0.075	0.125
4-Hydroxybenzaldehyde	0.300	0.475	0.750
4-Hydroxycinnamic acid (C)	0.075	0.163	0.625
4-Hydroxycinnamic acid (D)	0.075	0.163	0.625
4-Hydroxycinnamic acid (E)	0.075	0.163	0.625

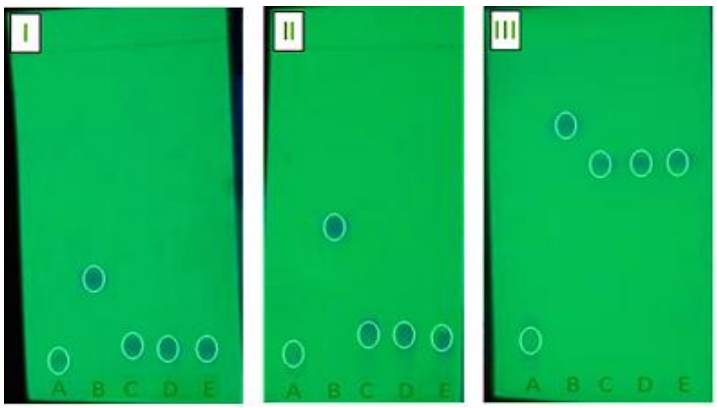

Figure 2. TLC analysis of 4-hydroxycinnamic acid compared to 4-hydroxybenzaldehyde, and malonic acid using various eluent; (A) malonic acid, (B) 4-hydroxybenzaldehyde, and (C, D, E) 4-hydroxycinnamic acid obtained from different reflux time 3, 5, and 7 hours, respectively; eluent I = *n*-hexane: ethyl acetate (2:1); eluent II = chloroform: ether (3:1); eluent III = chloroform: acetone: acetic acid = (10: 5: 0.5). TLC plate was detected under UV_{254}.

The infrared spectrum of the isolated condensation product (**Figure 3**) provides crucial diagnostic evidence for the presence of target functional groups, based on characteristic vibrational wavelengths. Parsing the infrared data enables the identification of specific absorption coordinates, with each unique peak position reflecting the structural environment of the synthesized molecule. The recording displays a sharp, intense band centered at 1674.21 cm^{-1}, confirming the presence of a C=O stretching vibration arising from the carboxylic acid (-COOH) terminus, which constitutes a primary diagnostic marker for cinnamic acid backbones. Two distinct absorption bands centered at 3387.00 cm^{-1} are assigned to the stretching vibrations of the phenolic -OH functional groups. The spectrum also exhibits a distinct peak at 3024.38 cm^{-1}, which corresponds to the sp2 hybrid C-H stretching vibrations of the aromatic ring core. Furthermore, the sharp, medium-intensity band appearing at 1627.21 cm^{-1} confirms the presence of the alkenic C=C bond within the conjugated α,β-unsaturated framework. These spectral assignments correlate with data published by Fang *et al.*[25], who mapped the characteristic -OH and alkenic C=C networks of functionalized 4-hydroxycinnamic acid at 3381 cm^{-1} and 1672 cm^{-1}, respectively.

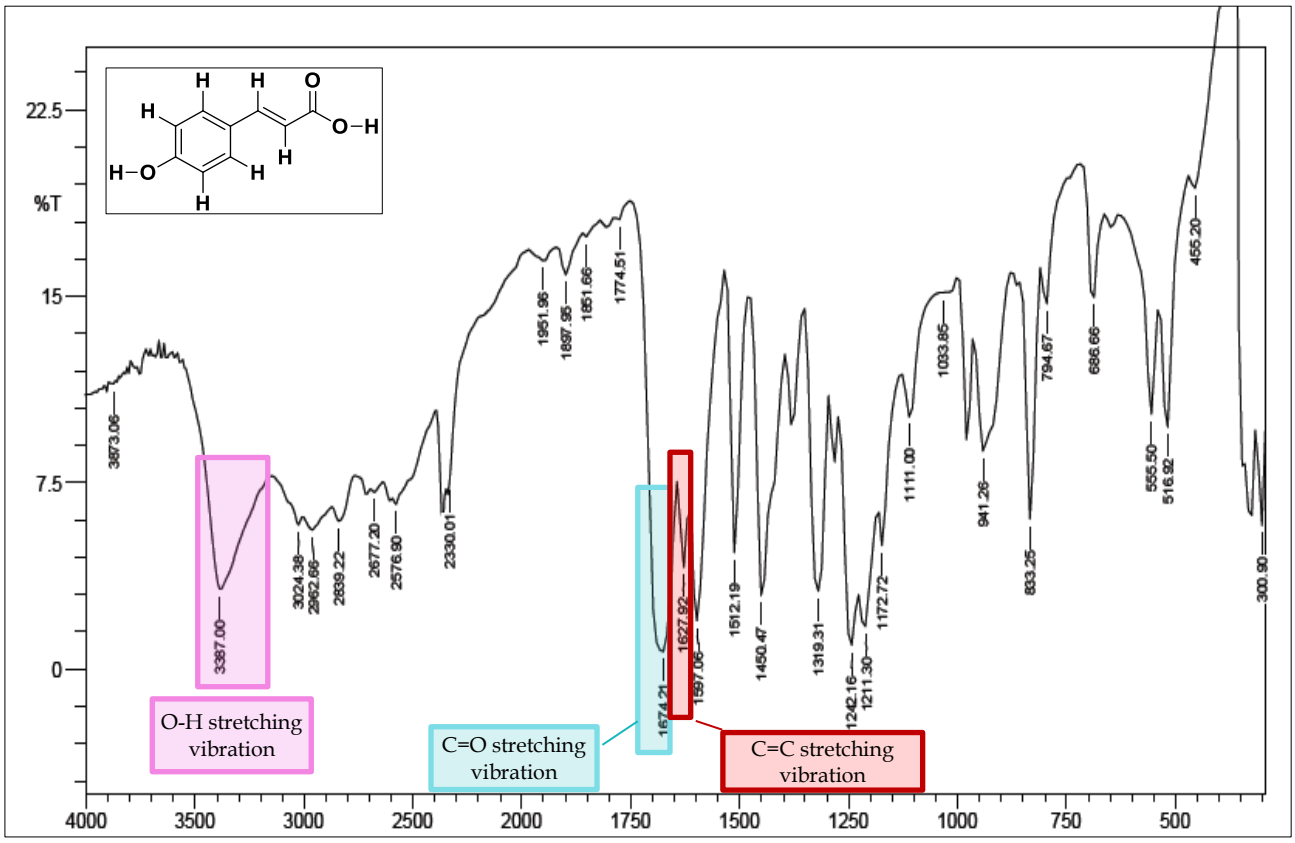

Figure 3. Infrared spectrum of 4-hydroxycinnamic acid (featuring O-H stretching vibration, C=O stretching vibration, and C=C stretching vibration markers).

Nuclear magnetic resonance spectroscopy remains an essential tool for parsing the precise structural architecture of organic frameworks, providing detailed insights into phase dynamics, conformational states, and configurational shifts[26]. Applying an external magnetic field to the target nuclei induces a characteristic resonance frequency that drives core-level energy-level transitions. The resulting δ values are highly sensitive to the surrounding electronic environment, meaning that atoms in chemically equivalent spaces within symmetric molecules experience identical shielding and generate overlapping signals[27]. In this study, high-resolution NMR experiments were performed to validate the carbon-hydrogen connectivity of the isolated 4-hydroxycinnamic acid. Proton and carbon spectral arrays were acquired using both acetone-*d6* (A) and DMSO-*d6* (B) as dissolving matrices to cross-reference solvent-dependent behaviors, with the extracted values collated in **Table III**. The corresponding ^{1}H-NMR traces recorded across both deuterated solvent environments are displayed sequentially in **Figure 4**.

Table III. Summarized NMR spectral data of 4-hydroxycinnamic acid.

Structure	Spectral data	
	Acetone-d_6	**DMSO-d_6**
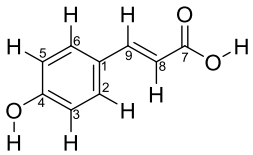	^{1}H-NMR (300 MHz, Acetone-d_6) δ_H 7.62 (d, J = 15.9 Hz, 1H), 7.57 – 7.47 (m, 2H), 6.94 – 6.84 (m, 2H), 6.34 (d, J = 16.0 Hz, 1H)[a]	^{1}H-NMR (300 MHz, DMSO-d_6) δ_H 7.56 – 7.44 (m, 3H), 6.84 – 6.73 (m, 2H), 6.28 (d, J = 15.9 Hz, 1H)[b]
	^{13}C-NMR (75 MHz, Acetone-d_6) δ_C 168.9, 160.5, 145.9, 130.9, 126.9, 116.6, 115.5[a]	^{13}C-NMR (75 MHz, DMSO-d_6) δ_C 168.1, 159.7, 144.3, 130.2, 125.4, 115.9, 115.5[b]

Note: [a,b] Spectral data were collected in acetone-*d6* and DMSO-*d6*, respectively.

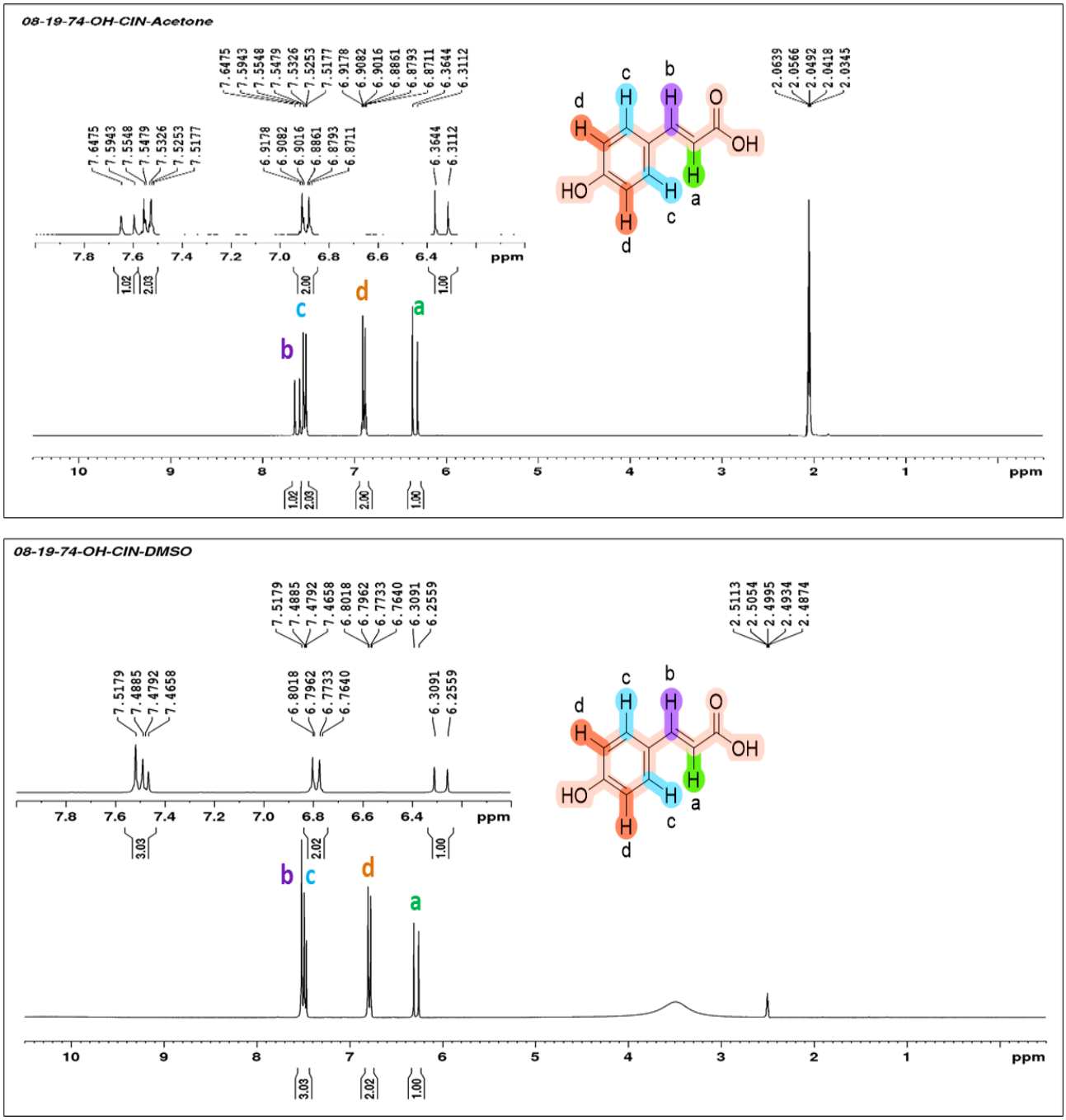

Figure 4. ^{1}H-NMR spectra of 4-hydroxycinnamic acid in (top) acetone-*d6* and (bottom) DMSO-*d6*.

As illustrated in **Figure 4**, the proton environments of the 4-hydroxycinnamic acid product were successfully resolved using both deuterated acetone and DMSO. Both spectra exhibit diagnostic splitting patterns in the aromatic region between 6.2 and 7.8 ppm, confirming the presence of the conjugated phenyl proton matrix. Observable variances in precise chemical

shift positions between the two traces reflect the influence of solvent polarity on local nuclear shielding dynamics. Specifically, the proton analysis conducted in acetone-*d6* resolved the phenyl ring protons as symmetric multiplet signals spanning 7.57–7.47 ppm and 6.94–6.84 ppm. Crucially, two sharp doublet signals appearing at 7.63 ppm and 6.34 ppm are explicitly tied to the trans-configured olefinic protons of the α,β-unsaturated chain, with the calculated J values spanning 15.9 to 16.0 Hz confirming the expected trans (*E*) geometry. When the sample was analyzed in DMSO-*d6*, one of the olefinic doublet signals shifted downfield and overlapped with the aromatic multiplet block, resolving as a combined multiplet integrating to three protons (δ_H = 7.56–7.44 ppm). Additionally, the highly exchangeable acidic carboxylic and phenolic hydroxyl protons were attenuated due to background trace moisture or active proton exchange with the deuterated solvent media. These values track historical literature data using acetone-*d6*, which placed the characteristic trans-olefinic alkene protons at 7.61 ppm and 6.34 ppm[24].

Regarding the carbon framework, the ^{13}C-NMR profiles of the 4-hydroxycinnamic acid were similarly traced in both DMSO-*d6* (A) and acetone-*d6* (B), as shown in **Figure 5**. The carbon trace acquired in acetone-*d6* shows a distinctive downfield carbonyl signal at 168.12 ppm, corresponding to the acid functionality, which shifts to 168.89 ppm when evaluated in DMSO-*d6*. Additionally, a cluster of carbon resonances in the 115–160 ppm range maps the positions of the aromatic and conjugated alkene carbon centers. These carbon position metrics align with historical literature controls[24]. Taken together, the ^{13}C spectral datasets provide robust corroboration of the structural preservation of the core aromatic and carbonyl elements, matching the expected spectral pattern of pure cinnamic acid derivatives.

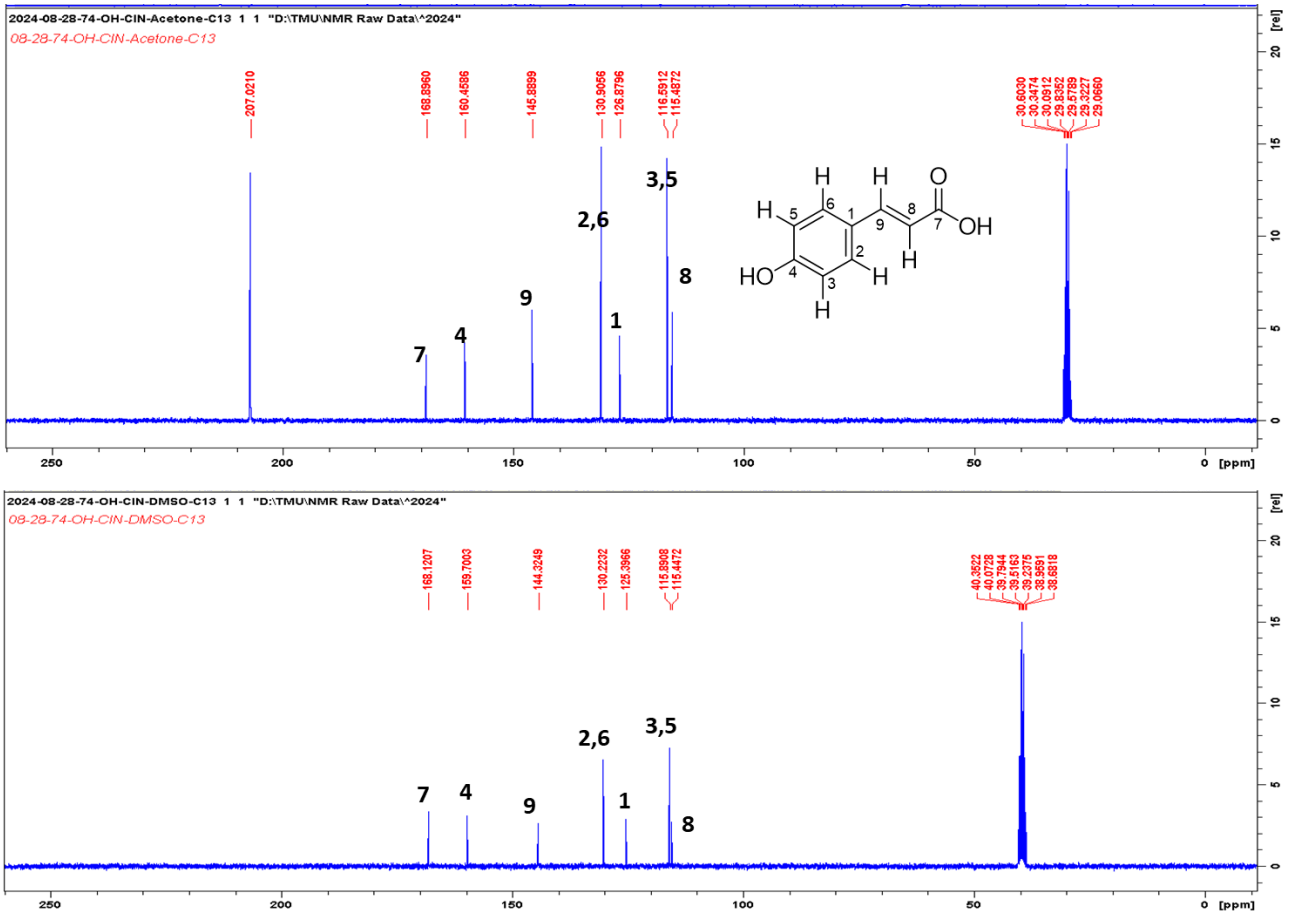

Figure 5. ^{13}C-NMR spectra of 4-hydroxycinnamic acid in (top) acetone-*d6* and (bottom) DMSO-*d6*.

Following structural validation, the purity profile of the synthesized crystalline compound was quantitatively evaluated using HPLC under the isocratic conditions detailed in the experimental section. As illustrated in the chromatogram in **Figure 6**, the synthesized 4-hydroxycinnamic acid sample exhibits a dominant primary peak at 12.224 minutes, confirming it as the primary component. This peak exhibits a sharp, highly symmetrical profile, indicating excellent sample homogeneity. The analytical trace also reveals two minor background peaks resolving at 20.250 and 22.512 minutes, which reflect trace

secondary impurities within the matrix. The absence of additional unexpected peak clusters supports the high purity of the isolated target compound.

Due to its highly polar nature and minimal interaction with the reverse-phase stationary phase, the injection solvent (DMSO) elutes early in the initial dead volume window (typically around 3–5 minutes) and manifests as a broad, irregular solvent front peak at high concentrations. In accordance with standard analytical protocols, these solvent front signals were excluded from the final purity calculations[28]. Consequently, using integrated peak area analysis, the final purity value of the synthesized 4-hydroxycinnamic acid was calculated to be approximately 97.99%. This high value confirms the efficiency and reproducibility of the condensation and downstream purification protocols. These combined analytical findings confirm that the selected reaction parameters and isolation steps successfully yielded a high-purity product suitable for subsequent applications.

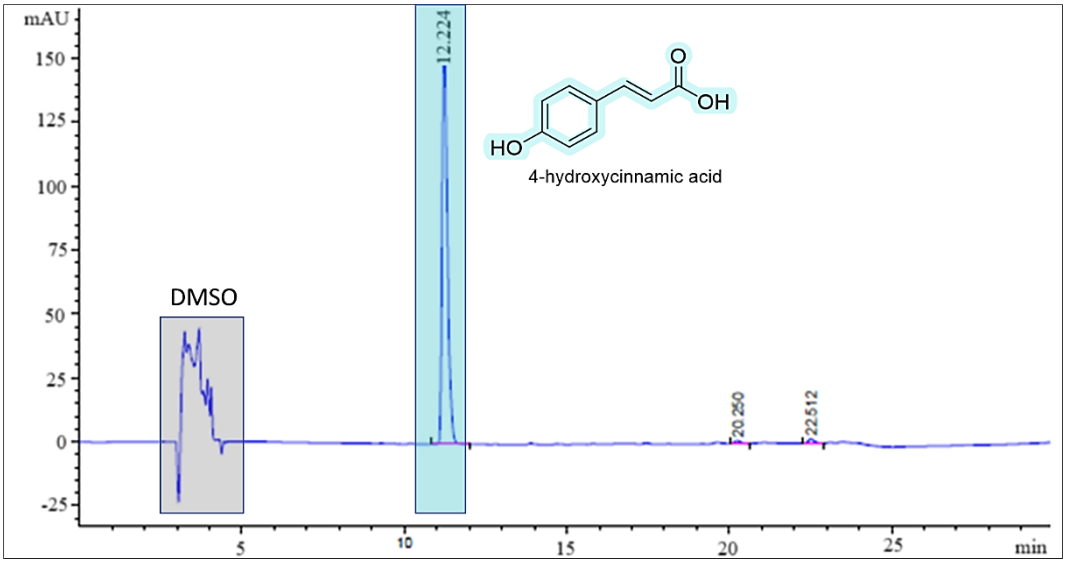

Figure 6. HPLC analysis of 4-hydroxycinnamic acid.

CONCLUSION

The synthesis of 4-hydroxycinnamic acid was successfully achieved via a Knoevenagel-Doebner condensation of malonic acid and 4-hydroxybenzaldehyde. Comparative evaluation of 3-, 5-, and 7-hour reflux durations showed that a 5-hour reaction time yields the optimal 66.78% yield, providing sufficient activation energy while preventing product degradation. By leveraging a pyridine-piperidine catalytic system under mild reflux conditions, this benchtop method offers high efficiency without specialized microwave-assisted apparatus. Structural confirmation via TLC, FTIR, and NMR verified the target molecular configuration, while HPLC analysis confirmed an excellent final product purity of 97.99%. Overall, this optimized protocol combines high yields, high purity, and operational simplicity, establishing a practical, highly reproducible method for preparing 4-hydroxycinnamic acid suitable for downstream applications.

ACKNOWLEDGMENT

There is no external funding for this research.

AUTHORS' CONTRIBUTION

Conceptualization: Iin Narwanti
Data curation: -
Formal analysis: Iin Narwanti, Fahmi Humaidi Abdillah
Funding acquisition: -

Investigation: Iin Narwanti, Fahmi Humaidi Abdillah
Methodology: -
Project administration: -
Resources: -
Software: -
Supervision: -
Validation: -
Visualization: -
Writing - original draft: Iin Narwanti, Fahmi Humaidi Abdillah
Writing - review & editing: Iin Narwanti

DATA AVAILABILITY

None.

CONFLICT OF INTEREST

The authors declared no conflict of interest related to this research.

REFERENCES

1. Li X, Hu Y, He B, Li L, Tian Y, Xiao Y, Shang H, Zou Z. Design, synthesis and evaluation of ursodeoxycholic acid-cinnamic acid hybrids as potential anti-inflammatory agents by inhibiting Akt/NF-κB and MAPK signaling pathways. Eur J Med Chem. 2023;260:115785. DOI: 10.1016/j.ejmech.2023.115785; PMID: 37678142.

2. Gunia-Krzyżak A, Słoczyńska K, Popiół J, Koczurkiewicz P, Marona H, Pękala E. Cinnamic acid derivatives in cosmetics: current use and future prospects. Int J Cosmet Sci. 2018;40(4):356-66. DOI: 10.1111/ics.12471; PMID: 29870052.

3. Mohammadabadi T, Jain R. Cinnamon: a nutraceutical supplement for the cardiovascular system. Arch Med Sci Atheroscler Dis. 2024;9:e72-81. DOI: 10.5114/amsad/184245; PMID: 38846056; PMCID: PMC11155465.

4. Letizia CS, Cocchiara J, Lapczynski A, Lalko J, Api AM. Fragrance material review on cinnamic acid. Food Chem Toxicol. 2005;43(6):925-43. DOI: 10.1016/j.fct.2004.09.015; PMID: 15811573.

5. Nouni C, Theodosis-Nobelos P, Rekka EA. Antioxidant and Hypolipidemic Activities of Cinnamic Acid Derivatives. Molecules. 2023;28(18):6732. DOI: 10.3390/molecules28186732; PMID: 37764507; PMCID: PMC10535275.

6. dos Santos DM, Sanches MP, Poffo CM, Parize AL, Darelli GJS, de Lima VR. Syringic and cinnamic acids antiradical/antioxidant activities as R. ferruginea extract components and membrane physico-chemical influence. J Mol Struct. 2020;1220:128749. DOI: 10.1016/j.molstruc.2020.128749.

7. Perković I, Raić-Malić S, Fontinha D, Prudêncio M, de Carvalho LP, Held J, et al. Harmicines - harmine and cinnamic acid hybrids as novel antiplasmodial hits. Eur J Med Chem. 2020;187:111927. DOI: 10.1016/j.ejmech.2019.111927; PMID: 31812035.

8. Romagnoli R, Oliva P, Prencipe F, Manfredini S, Germanò MP, De Luca L, et al. Cinnamic acid derivatives linked to arylpiperazines as novel potent inhibitors of tyrosinase activity and melanin synthesis. Eur J Med Chem. 2022;231:114147. DOI: 10.1016/j.ejmech.2022.114147; PMID: 35114540.

9. Rodrigues MP, Tomaz DC, de Souza LA, Onofre TS, de Menezes WA, Almeida-Silva J, et al. Synthesis of cinnamic acid derivatives and leishmanicidal activity against Leishmania braziliensis. Eur J Med Chem. 2019;183:111688. DOI: 10.1016/j.ejmech.2019.111688; PMID: 31542714.

10. Huang S, Liu W, Li Y, Zhang K, Zheng X, Wu H, et al. Design, Synthesis, and Activity Study of Cinnamic Acid Derivatives as Potent Antineuroinflammatory Agents. ACS Chem Neurosci. 2021;12(3):419-29. DOI: 10.1021/acschemneuro.0c00578; PMID: 33439002.

11. Liang C, Pei S, Ju W, Jia M, Tian D, Tang Y, et al. Synthesis and in vitro and in vivo antitumour activity study of 11-hydroxyl esterified bergenin/cinnamic acid hybrids. Eur J Med Chem. 2017;133:319-28. DOI: 10.1016/j.ejmech.2017.03.053; PMID: 28395218.

12. Xu CC, Deng T, Fan ML, Lv WB, Liu JH, Yu BY. Synthesis and in vitro antitumor evaluation of dihydroartemisinin-cinnamic acid ester derivatives. Eur J Med Chem. 2016;107:192-203. DOI: 10.1016/j.ejmech.2015.11.003; PMID: 26595184.

13. Almeer RS, Alnasser M, Aljarba N, AlBasher GI. Effects of Green cardamom (Elettaria cardamomum Maton) and its combination with cyclophosphamide on Ehrlich solid tumors. BMC Complement Med Ther. 2021;21(1):133. DOI: 10.1186/s12906-021-03305-2; PMID: 33926427; PMCID: PMC8086365.

14. Indriyanti E, Prahasiwi MS. Synthesis of cinnamic acid based on perkin reaction using sonochemical method and its potential as photoprotective agent. JKPK J Kimia Pendidikan Kimia. 2020;5(1):54-61. DOI: 10.20961/jkpk.v5i1.38136.

15. Hatsuda M, Kuroda T, Seki M. An improved synthesis of (E)-cinnamic acid derivatives via the Claisen–Schmidt condensation. Synth Commun. 2003;33(3):427-34. DOI: 10.1081/SCC-120015773.

16. van Schijndel J, Canalle LA, Molendijk D, Meuldijk J. The green Knoevenagel condensation: solvent-free condensation of benzaldehydes. Green Chem Lett Rev. 2017;10(4):404-11. DOI: 10.1080/17518253.2017.1391881.

17. Nagalakshmi K, Diwakar BS, Govindh B, Reddy PG, Venu R, Bhargavi I, et al. A simple and straightforward synthesis of cinnamic acids and ylidene malononitriles via knoevenagel condensation employing DABCO as catalyst. Asian J Chem. 2017;29(7):1561-4. DOI: 10.14233/ajchem.2017.20575.

18. Lee GS, Widjaja A, Ju YH. Enzymatic synthesis of cinnamic acid derivatives. Biotechnol Lett. 2006;28(8):581-5. DOI: 10.1007/s10529-006-0019-2; PMID: 16614896.

19. Lin CI, McCarty RM, Liu HW. The Enzymology of Organic Transformations: A Survey of Name Reactions in Biological Systems. Angew Chem Int Ed Engl. 2017;56(13):3446-89. DOI: 10.1002/anie.201603291; PMID: 27505692; PMCID: PMC5477795.

20. Chiriac CI, Tanasa F, Onciu M. A novel approach in cinnamic acid synthesis: direct synthesis of cinnamic acids from aromatic aldehydes and aliphatic carboxylic acids in the presence of boron tribromide. Molecules. 2005;10(2):481-7. DOI: 10.3390/10020481; PMID: 18007319; PMCID: PMC6147640.

21. van Beurden K, de Koning S, Molendijk D, van Schijndel J. The Knoevenagel reaction: a review of the unfinished treasure map to forming carbon–carbon bonds. Green Chem Lett Rev. 2020;13(4):349-64. DOI: 10.1080/17518253.2020.1851398.

22. Rioux B, Peyrot C, Mention MM, Brunissen F, Allais F. Sustainable Synthesis of p-Hydroxycinnamic Diacids through Proline-Mediated Knoevenagel Condensation in Ethanol: An Access to Potent Phenolic UV Filters and Radical Scavengers. Antioxidants. 2020;9(4):331. DOI: 10.3390/antiox9040331; PMID: 32325641; PMCID: PMC7222392.

23. Julianus J, Luckyvano E. Sintesis asam sinamat dari benzaldehida dan asam malonat dengan katalis dietilamina. J Farm Sains Komunitas. 2014;11(1):1-6. DOI: 10.24071/jpsc.0061

24. Mouterde LMM, Allais F. Corrigendum: Microwave-Assisted Knoevenagel-Doebner Reaction: An Efficient Method for Naturally Occurring Phenolic Acids Synthesis. Front Chem. 2018;6:568. DOI: 10.3389/fchem.2018.00568; PMID: 30519557; PMCID: PMC6256712.

25. Fang X, Hu Y, Yang G, Shi W, Lu S, Cao Y. Improving physicochemical properties and pharmacological activities of ternary co-amorphous systems. Eur J Pharm Biopharm. 2022;181:22-35. DOI: 10.1016/j.ejpb.2022.10.008; PMID: 36283631.

26. Oladipo SD, Yusuf TL, Zamisa SJ, Shapi M, Ajayi TJ. Synthesis, crystal structure, Hirshfeld surface analysis and DFT studies of N-(2,6-diisopropylphenyl)-1-(4-methoxyphenyl) methanimine. J Mol Struct. 2021;1241:130620. DOI: 10.1016/j.molstruc.2021.130620.

27. Aiswarya P, Jayavarthanan T, Periandy S, Suresh S, Soundhariya S. Molecular structural analysis, conformers and spectral (FT-IR, FT-Raman, NMR and UV-Visible), Importance of solvent role in molecular, ADME and molecular docking investigation on alpha-cyano-4-hydroxycinnamic acid. Chem Phys Impact. 2023;7:100353. DOI: 10.1016/j.chphi.2023.100353.

28. Narwanti I, Yu ZY, Sethy B, Zheng PL, Cheng LH, Tsai KK, et al. Quinoline-5,8-dione CDC25 inhibitors: Potent anti-cancer agents in leukemia and patient-derived colorectal organoids. Eur J Med Chem. 2026;301:118215. DOI: 10.1016/j.ejmech.2025.118215; PMID: 41045697.